

Scanning Electrochemical Microscopy Applied to Metals and Coatings

Subjects: Electrochemistry | Materials Science, Characterization & Testing

Contributor: Ricardo Souto, Juan Santana, Javier Izquierdo Pérez

Scanning electrochemical microscopy (SECM) is a scanning probe microscope (SPM) technique based on electrochemical principles that allows chemical imaging of materials with spatial resolution. The movement of a microelectrode (ME) in close proximity to the interface allows the application of various experimental procedures that can be classified into amperometric and potentiometric operations depending on either sensing faradaic currents or probe potential values due to concentration distributions resulting from the corrosion process, as sketched in. In addition, alternating current signals can be applied to the ME, leading to AC-operation modes.

Keywords: scanning electrochemical microscopy ; corrosion protection ; coating degradation

1. Experimental Design for scanning electrochemical microscopy (SECM) Operation

There are several important factors to be considered when designing a SECM experiment. The most important ones are the nature and geometry of the tip that will determine the spatial and chemical resolutions of the measurement, as well as the type of substrate and mediator, and the solvent to be employed. It was provided that the main experimental design factors related to the application of SECM to the analysis of metals and alloys, as well as these when covered by surface layers or coating systems. All the information has been organized in tables in order to simplify the presentation of the available resources and their easier comparison elsewhere ^[1]. It was provided a brief description of the main aspects related to the features in the next sub-sections. It must be noted that method validation will not be discussed here as it is beyond the reach, but a relevant on the topic has been recently presented by Izquierdo et al. ^[2].

1.1. SECM Instrumentation

SECM is a scanning probe microscope (SPM) technique based on electrochemical principles ^[3]. The movement of a microelectrode (ME) in close proximity to the interface allows the application of various experimental procedures that can be classified into amperometric and potentiometric operations depending on either sensing faradaic currents or probe potential values due to concentration distributions resulting from the corrosion process, as sketched in **Figure 1**. In addition, alternating current signals can be applied to the ME, leading to AC-operation modes.

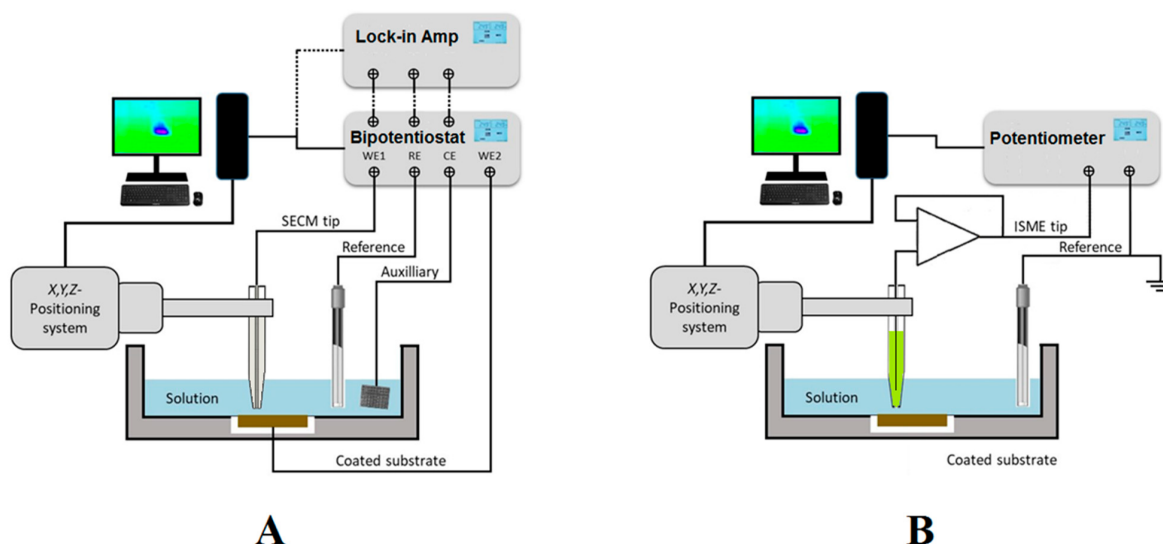


Figure 1. Sketches depicting the SECM set up and electrode connections for (A) amperometric and AC operations; and (B) potentiometric operation.

As sketched in **Figure 1A**, amperometric SECM operation is performed in a small electrochemical cell constituted by the tip, the counter electrode, the reference electrode, the substrate, and the solution. A bipotentiostat completes the SECM electrochemical setup together with the electrochemical cell, and it can be used to independently control the potential (bias) of the tip and the substrate, although the latter can also be left unbiased at its spontaneous corrosion potential in the environment. Next, a micropositioner is driven by stepper motors or piezoelectric elements to achieve the movement of the tip in the X, Y, and Z directions for exploring the substrate with submicrometric resolution. The experimental setup is completed with the interface, display system, and computer that records the current at the tip (and eventually the substrate when polarized by the bipotentiostat) as a function of tip position or the potential of the corresponding working electrode.

AC modes are available by attaching a lock-in amplifier or a frequency response analyser (FRA) to the bipotentiostat, as shown in **Figure 1A**. 4D AC-SECM mode involves the electrochemical imaging of the AC components of the current signal flowing at the tip (for example, admittance and phase angle) ^[4], whereas impedance spectra can be generated at the scanning electrochemical impedance microscope (SEIM) by combining the local current and potential signals ^[5].

Alternately, potentiometric operation can be performed by measuring local potential signals in a two-electrode cell configuration, as sketched in **Figure 1B**. In this situation, a high input impedance operational amplifier must be introduced between the electrode connections in the electrochemical cell before they are driven to the bipotentiostat or the potentiometer unit employed as electrochemical interface ^[6]. Ion-selective microelectrodes (ISMEs) are used as SECM probes instead of the active tip surfaces employed in amperometric and AC modes. Although potentiometric SECM, also known as the scanning ion selective electrode technique (SIET) in some publications, has usually been performed using two separate electrodes in the electrochemical cell, as sketched in **Figure 1B**, it was demonstrated that such an arrangement contributes to big uncertainties in the measurement of local potential values in systems undergoing corrosion reaction, due to the high electrical fields developed in the electrolyte by galvanic pair systems ^[7]. The use of internal reference electrodes built inside the ion-selective electrode tip should be mandatory in order to overcome this reported limitation ^{[8][9]}. Another limitation arises from the rather slow equilibration time required to establish a stationary Donnan potential in the ion-selective membrane of the ISME, effectively limiting the resolution of the chemical images that can be recorded using this operation mode, which is often reduced to a few 2D line scans ^[10], although new imaging procedures involving the construction of 3D pseudo-maps have recently become available ^[11].

A summary of the SECM instruments and the analytical figures of merit necessary for adequate description of the experiments and reproducibility are focused elsewhere ^[4].

1.2. Tips Used for Amperometric Operation

Tips employed in amperometric SECM are active microelectrodes (MEs) of a critical dimension below 25 μm for conditioning the mass transport of a redox species from the solution toward the electrode, which are used to characterize coatings and/or thin surface layers applied on metals without requiring any additional modification ^[12]. In SECM, the most employed tip is built using a platinum wire of different diameters, followed by gold and carbon microwires or fibres, although antimony- and iridium-based tips have been occasionally employed due to the dual amperometric/potentiometric potential of their oxides ^{[13][14]}.

For the tip fabrication, usually a metal microdisk (e.g., Pt) is sealed into a glass capillary and tapered to a conical shape. Then, it is polished with graded alumina powder (or similar) of different sizes in order to expose a disk-shaped electrode with an active surface for the redox reaction and is fully characterized by recording a cyclic voltammogram of a known electroactive species (e.g., a redox mediator) added to the test solution, as it is exemplified in **Figure 2** of the oxidation of ferrocene-methanol on a Pt ME.

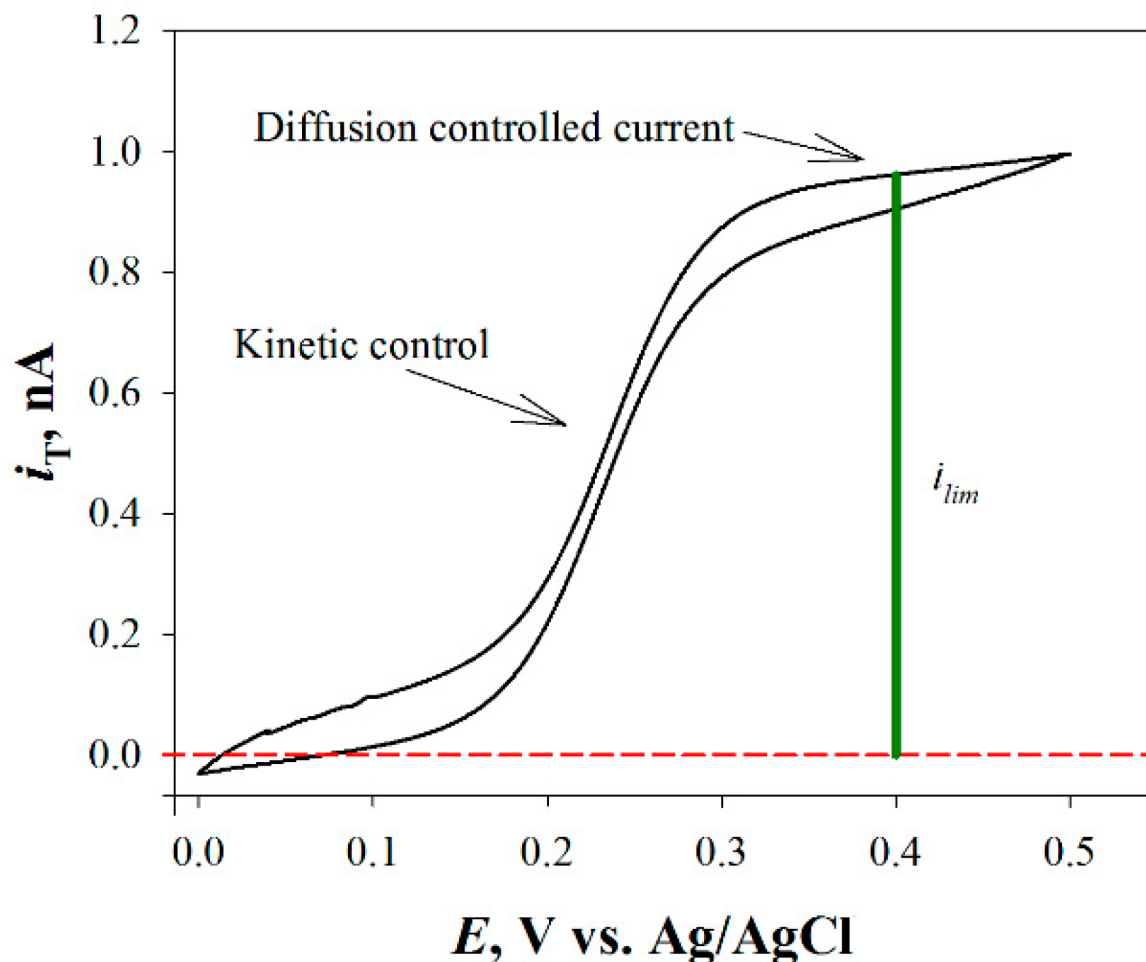


Figure 2. Cyclic voltammetry curve for ferrocene-methanol (i.e., the most employed redox mediator) on a Pt ME.

1.3. Redox Mediators

A redox mediator is an electroactive molecule, atom, or ion that can be reduced or oxidized. Mediators are classified as direct and indirect redox mediators depending on whether the species is already present in the solution (e.g., O_2) or has to be added to the solution to perform the experiment (e.g., ferrocene-methanol, FcMeOH). The latter is needed to monitor either insulating or poorly-conductive substrates, thus reflecting only topographical and/or chemical reactivity changes along a surface, respectively, as sketched in **Figure 3**. Redox mediators may also be added for precise tip positioning of the tip relative to the substrate by recording the changes in the tip current while approaching the substrate, as well as to locate sites of different reactivity on the substrate (cf. **Figure 3**). Normally, when a redox mediator species is added to the solution, a low concentration (approximately in mM values) is used. However, more strictly, the concentration of the mediator must be chosen by taking into account its reaction rate at the substrate. Besides, it may be necessary to adjust the pH.

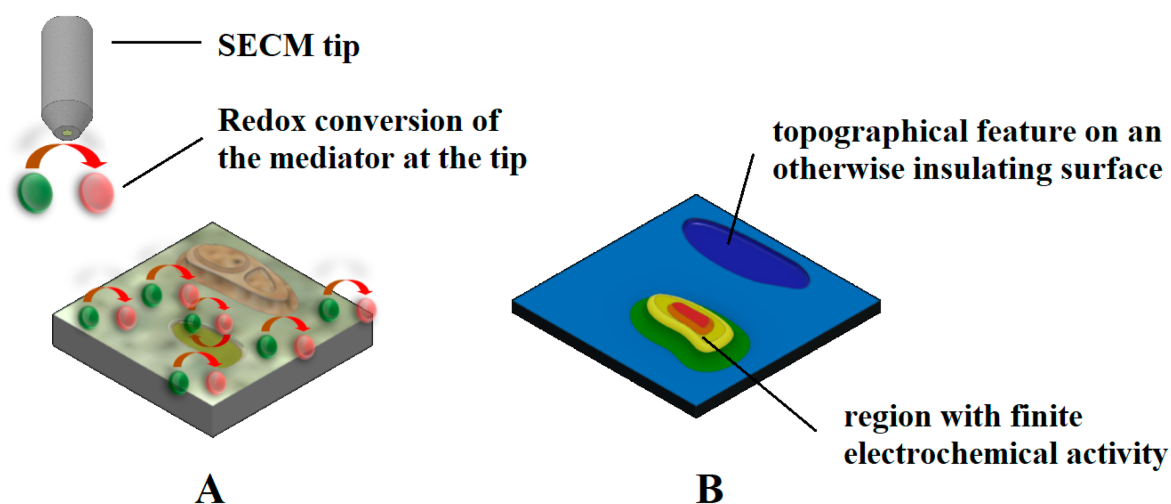


Figure 3. Sketches depicting: (A) the redox conversion of an electrochemical mediator at the amperometric tip of SECM over a mostly insulating surface, whereas the redox mediator regeneration solely occurs in a region exhibiting

electrochemical reactivity; and (B) the current measured at the tip, which contains information on the topography of the sample (i.e., blue color palette) eventually coupled with a region showing a heterogeneous chemical reactivity distribution (red and yellow color palette).

The selection of a certain redox mediator for a given experiment is a critical issue for a successful experiment and depends on several factors, such as:

- The nature of the sample studied;
- The nature of the mediator (chemical stability, redox potential, photostability, toxicity, thermal stability, and solubility in the solution to be tested); and
- The mode of operation to use in SECM.

A broad classification of redox mediator systems for the investigation of electrochemical corrosion processes can be made by considering whether the species is added to the test environment for imaging (ideal redox mediator system) or whether it is a certain chemical species that participates in the corrosion mechanism, although the latter frequently exhibits poorly reversible or even irreversible electron transfer reactions (for instance, the electroreduction of molecular oxygen) and highly variable concentration ranges. Since corrosion reactions on coated metals often expose insulating or poorly conductive layers to the electrolytic phase in which the SECM tip is moved, the use of corrosion-related mediators is limited to systems presenting either defects or cut edges, or low efficiencies of inhibition. In contrast, the addition of redox mediators that exhibit fast, simple, and highly reversible electron transfer reactions at the tip is preferred for non-defective and barrier-type layers and coatings, where the initiation of the corrosion reactions occurs in the buried interface formed by the metal and the surface layer. The information collected on the degradation process is obtained by observing morphological and topographical changes on the outer surface of the coating or film. An intermediate case occurs during the formation of inhibiting layers on metals by adsorption, because there is a gradual transition from an electrochemically active surface to a (quasi) insulating surface, making it possible to follow the time course of the charge transfer reaction at the surface^[15]. In this case, the main care must relate to the selection of a mediator having a redox potential close to the corrosion potential of the substrate, in order to minimize the effects of polarization of the substrate by the redox couple.

1.4. Tips Used for Potentiometric Operation

Passive tips (ISME) are employed in potentiometric SECM. Since ion activities are detected using ISME tips, without being consumed during the measurement, no interaction must occur with the sample surface. Although chemical selectivity is thus envisaged compared to amperometric operation, the selectivity of the probe is not always sufficiently high and it is necessary to be investigated in regards to other ions present in the system^[16]. Additionally, longer acquisition times are required for SECM measurement due to longer response times of the probes. When scanning rates similar to those typical for amperometric SECM operation are employed, the recorded images may exhibit significant aberration effects. Nevertheless, significant improvement has been achieved by combining dedicated scanning routines with mathematical deconvolution procedures ^{[17][18]}.

Potentiometric probes used in SECM can be classified into two broad categories, namely metal-based microsensors ^[19] and reference microelectrodes ^[20]. The first class of potentiometric microsensors take advantage of the passive properties of certain metal oxides that are primarily sensitive mainly to pH changes in the environment, such as antimony and iridium. Although the narrow potential range of stability of its metallic state in electrolyte solutions precludes its use as an electrode material with voltammetric techniques, it encompasses the potential range of O₂ electroreduction and therefore can be used in SECM for precise probe positioning ^{[21][22]}, which is a typical limitation of most passive potentiometric probes. In this way, the z-approach curves are recorded with the metal in the active state (for example, operating as a conventional amperometric SECM tip with redox mediators that are converted within the potential stability range of the elemental state of the tip metal), and then oxidized to produce the pH-sensitive metal oxide layer^[23]. In other cases, positioning is achieved with dual microelectrodes with the feedback mode by adding a redox mediator to the electrolyte ^{[14][24]}, a procedure that is described. Unfortunately, only a very small number of ion species can be detected using this type of microsensors (namely, H⁺, Ag⁺, and Cl⁻), and indeed they have only been used as pH microscopy when characterizing thin surface layers and coatings on metals.

The second type of passive potentiometric probes corresponds to ion-selective microelectrodes (ISMEs), which consist of a selective transducer (usually a membrane) that transfers the ion activity of a certain species occurring in the electrolyte phase to an electrical potential. The sensing membrane is a multicomponent solution (herein named cocktail) containing the ionophore, the polymeric matrix, the lipophilic ion exchanger, and the lipophilic salt. The ionophore is the component

that selectively forms a complex with the primary ion to be monitored, whereas the polymeric matrix accounts for the mechanical stability of the system. Since membranes must be immiscible with water, lipophilic components are employed.

2. Operation Modes

2.1. Feedback Modes

The feedback mode was one of the first operation modes employed in SECM^[25], and it is one of the most frequently employed modes due to its versatility. In this mode, the tip current (i_T) due to the redox conversion of a redox mediator is monitored, and its magnitude varies with the tip/substrate distance (d), the chemical nature of the mediator as well as the composition and conductivity of the electrolytic solution. A different potential value must be applied to the tip for each redox mediator. In the presence of a non-conductive substrate, the diffusion of the mediator is hindered and eventually blocked in the proximity of the substrate. That is, the faradaic current measured at the tip, i_T , gradually decreases while performing an approach of the tip to the substrate because the diffusion of the mediator towards the active area of the tip is hindered by the proximity of the substrate ($i_T < i_{T,\infty}$), and this behaviour is named negative feedback (see **Figure 4A**). Since the underlying metal is not in direct contact with the electrolyte medium for non-defective insulating coatings, the use of a redox mediator and its eventual development of a redox potential in the system produces no significant effect on the investigated system. Although the information provided by the technique has only spatial resolution (i.e., topography and morphology), this mode has found application for the investigation of transport phenomena through defect-less barrier organic coatings applied on metallic substrates leading to mechanistic information on water uptake ^{[26][27][28]} and lixiviation processes ^[29], as well as the detection of the early stages of coating blistering and delamination induced by ionic species such as chloride ^{[30][31][32][33]}.

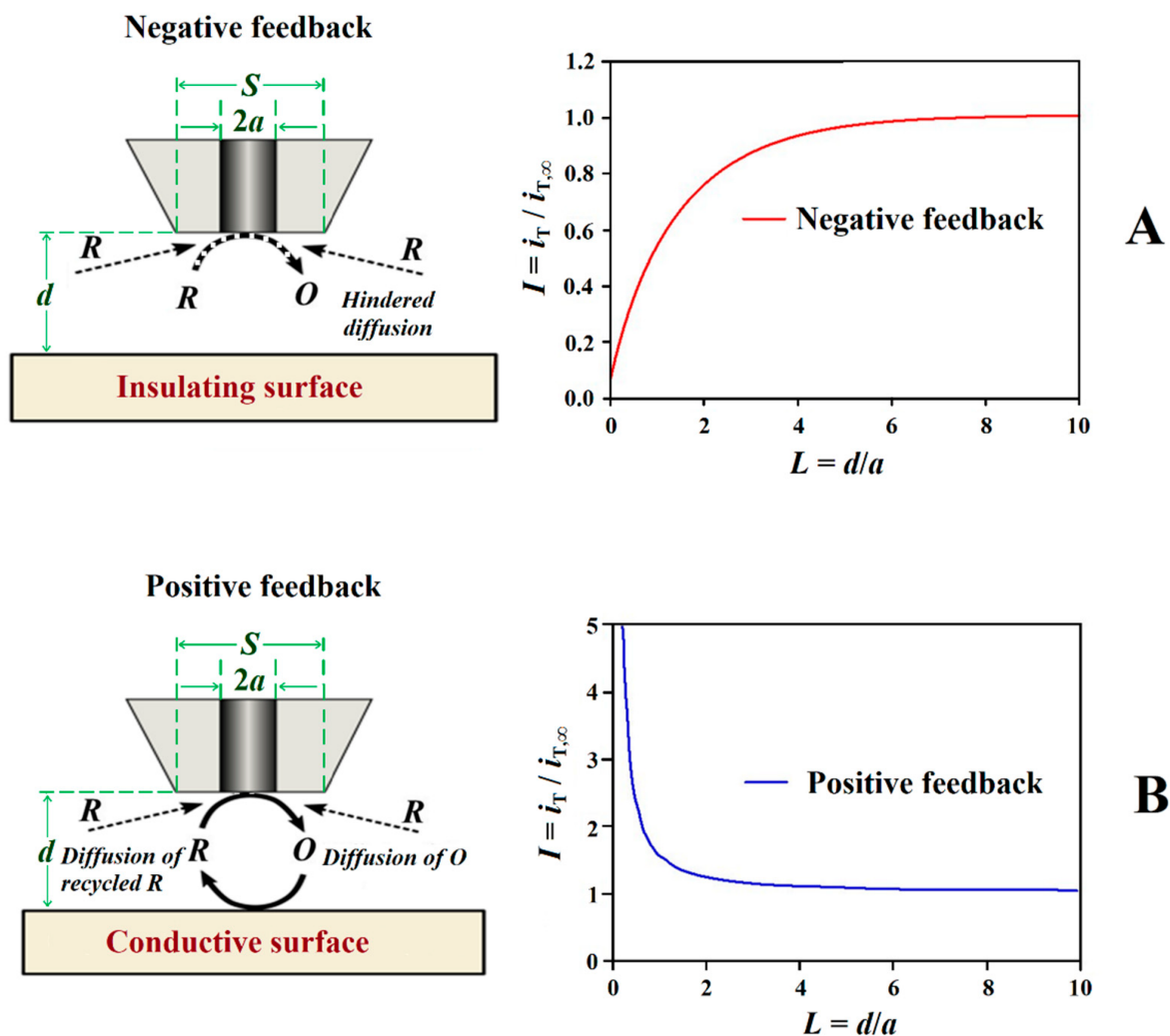


Figure 4. Schemes and shapes of Z-approach curves in the feedback mode of SECM. Types of feedback: (A) negative and (B) positive.

Conversely, if the surface of the sample is conductive, the mediator can be regenerated on it, and an increase of i_T can be observed ($i_T > i_{T,\infty}$) for smaller tip-substrate distances originating a positive feedback behaviour (cf. **Figure 4B**). For electrically insulating or conductive surfaces is possible thanks to the appearance of negative or positive feedback effects,

obtaining images of the surface that reflect the occurrence of defects in insulating coatings, including both inorganic and organic matrices, to be investigated [10][34][35][36]. Depending on the size of the tip, the measurement of i_T can thus provide information about sample topography and its electrical and chemical properties, allowing for the occurrence of defects ranging from pinholes to holidays and scratches, to be detected, as well as to monitor their evolution [34][35][36]. In brief, insulating regions produce changes in the current measured at the tip due to topographic changes that modify the transport regime of the redox mediator from the electrolyte bulk towards the tip, frequently interfering with the signal while scanning the substrate in close proximity. Conversely, regions in the substrate that are conductive and capable of regenerating the redox mediator produce an increase in current measured at the tip. It should be noted that, since the current response in feedback mode is highly dependent on tip-to-substrate distance, it is preferable to use as small a distance as possible (without crashing the tip) to increase sensitivity.

For the feedback operation mode, kinetic information can also be extracted from the experimental approach curves after taking in account the geometric factors of the tip^[37], which is of direct application for the determination of the rate constants associated with the formation of corrosion inhibitor layers on metals and their ageing by thickening or greater compactness^{[38][39][40][41]}. Additionally, the method has also been employed to gain information on the adsorption of the inhibitor molecules on the metal^[15].

2.2. Generation-Collection Modes

The term generation/collection mode encompasses two different modes of amperometric operations in SECM: tip generation/substrate collection (TG/SC) (see **Figure 5A,B**), and substrate generation/tip collection (SG/TC) (in **Figure 5C**), the main difference being the site at which the redox reaction employed for imaging occurs; either at the substrate or at the tip^[42]. Although the tip and the substrate both act as working electrodes, the corrosion processes at the substrate are sufficient to develop a spontaneous potential that sustains the reaction without the need to polarize the substrate^[43]. In this case, only the application of a potential to the SECM tip is necessary to measure the current flowing at the tip. An alternative situation occurs when the bipotentiostat is employed to set the substrate potential as well as the tip, since the instrument can be used to measure current in both the SECM tip and the substrate.

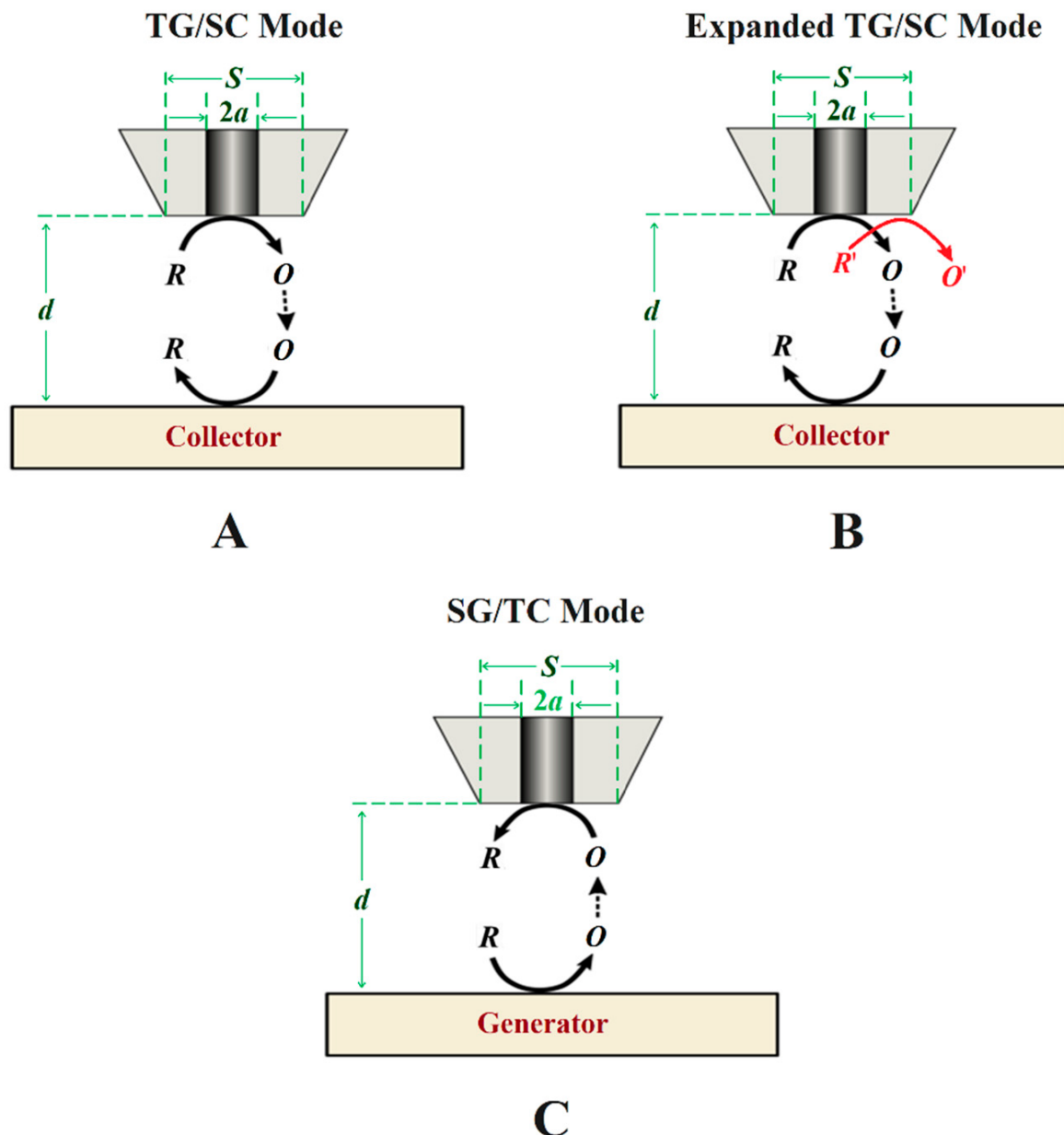


Figure 5. Schemes of generation-collection (G/C) modes of SECM. Types of G/C: (A) conventional tip generation and substrate collection, (B) bi-reaction tip generation and substrate collection, and (C) sample generation and tip collection.

In the TG/SC mode, the electroactive species that can be detected at the substrate is generated at the tip. In this case, the tip and the substrate must have different potentials, either using the bipotentiostat or by the substrate developing a different open circuit potential (OCP). A multireaction TG/SC mode was introduced by Leonard and Bard ^[44] in 2013 by using the redox conversion of two different species at the tip, as shown in **Figure 5B**. Depending on the potential required to reduce O to R or O' to R' at the substrate, if it is different for both reactions and a total collection efficiency of O from R can be set at the tip, then the current associated with each of the two reduction reactions can be separated. For corrosion systems, other possibilities for bi-reaction interfaces can include two oxidation reactions or a reduction combined with an oxidation.

In SG/TC, the current at the microelectrode arises from a species generated at the surface of the substrate (**Figure 5C**). This is the traditional G/C mode, and it has an important application for determining the reaction rates in function of the tip-to-substrate distance. If R reacts during its transport from the tip to the substrate, the relation between the current intensity at the substrate and at the tip becomes smaller and will greatly vary with the distance, d , and it can be used to obtain the rate constant of the homogeneous reaction.

2.3. Redox Competition Mode

The redox competition mode was introduced by Schuhmann and co-workers in 2006 ^[45] in a work related to catalysis. In this mode, the SECM tip and the substrate are polarized using the bipotentiostat. When the tip and the substrate are close to each other, they compete for the same redox species (see **Figure 6**), although the current is measured only at the tip. In a typical corrosion system formed by a metal covered by a non-conductive coating, the oxygen reduction current

measured at the SECM tip remains constant while the tip is scanned over the non-defective coating ^[46]. However, if a scratch is made through the coating system and the metal is exposed to the solution, the current measured at the SECM tip will decrease as the tip explores this active area because the redox species (e.g., oxygen) is consumed at both working electrodes ^[47], and the decrease observed can be correlated to the chemical activity of the substrate that corrodes after its direct exposure to the aggressive environment.

Redox Competition Mode

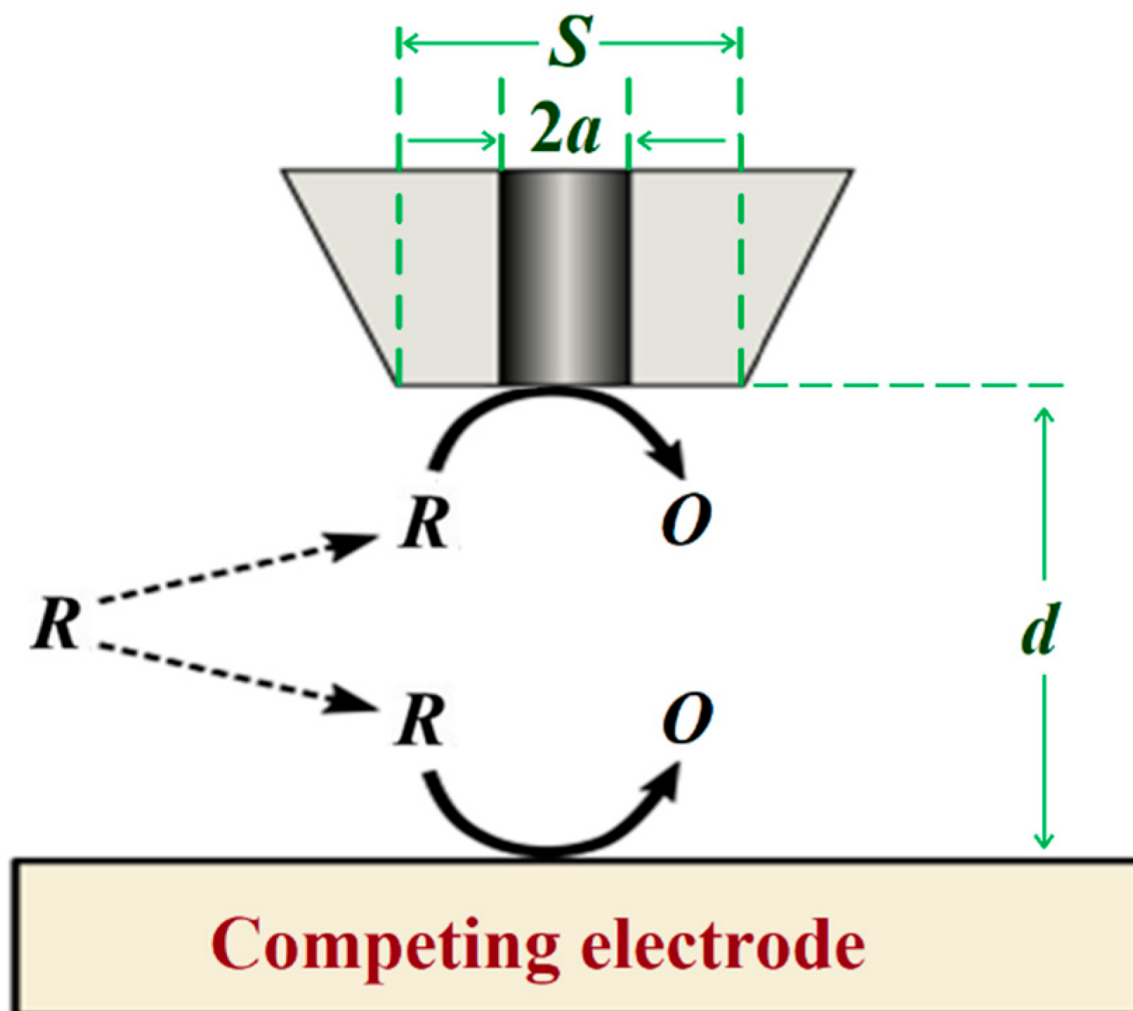


Figure 6. Scheme of the redox competition mode of SECM.

2.4. Combined Operation Modes

The signal recorded by the sensing probes of SECM consists of a complex combination of spatially-resolved information originating from the distance between the tip and the surface of the sample (i.e., sensitive to the morphology of the substrate) and of the actual chemical response due to the reactivity of the substrate, which in practice mainly limits its use to the characterization of flat surfaces and to the first stages of the formation of the surface film due to its progressive roughness with degradation. Although the morphological and chemical information may be ultimately convoluted in conventional SECM analysis, the first contribution can be considered constant for a flat surface, so that changes in probe response can be attributed to the chemical reactivity of the system. Unfortunately, highly reactive systems occurring in light-weight alloy materials, which rapidly develop layers of oxide products and gas evolution under common operating conditions, and those associated with the self-healing mechanisms of smart coatings containing nanoreservoirs for functionalized operation, do not exhibit flat surfaces. This feature is not a real limitation for the investigation of thin films on metals because their width dimensions are often much smaller than the size of the scanning probe, but it can make it difficult to characterize larger surface defects such as crevices or heterogeneous regions extending over a large surface compared to the tip dimensions such as those formed in welds. Notwithstanding, efficient measurement strategies have been developed to construct SECM surface images by combining separate images of smaller regions ^[48].

To overcome this limitation imposed by the convolution of topographic information and chemical activity in the signal measured at the tip, a multi-scale electrochemical methodological procedure can be performed to deconvolute chemical information relevant to corrosion reactions and protection mechanisms in such complex systems can be performed [49]. Souto and coworkers developed a quite simple and systematic methodological procedure involving the combined use of various operation modes in amperometric SECM to learn defects in organic coatings of width and depth dimensions greater than those of the tip [50], as illustrated in **Figure 7**.

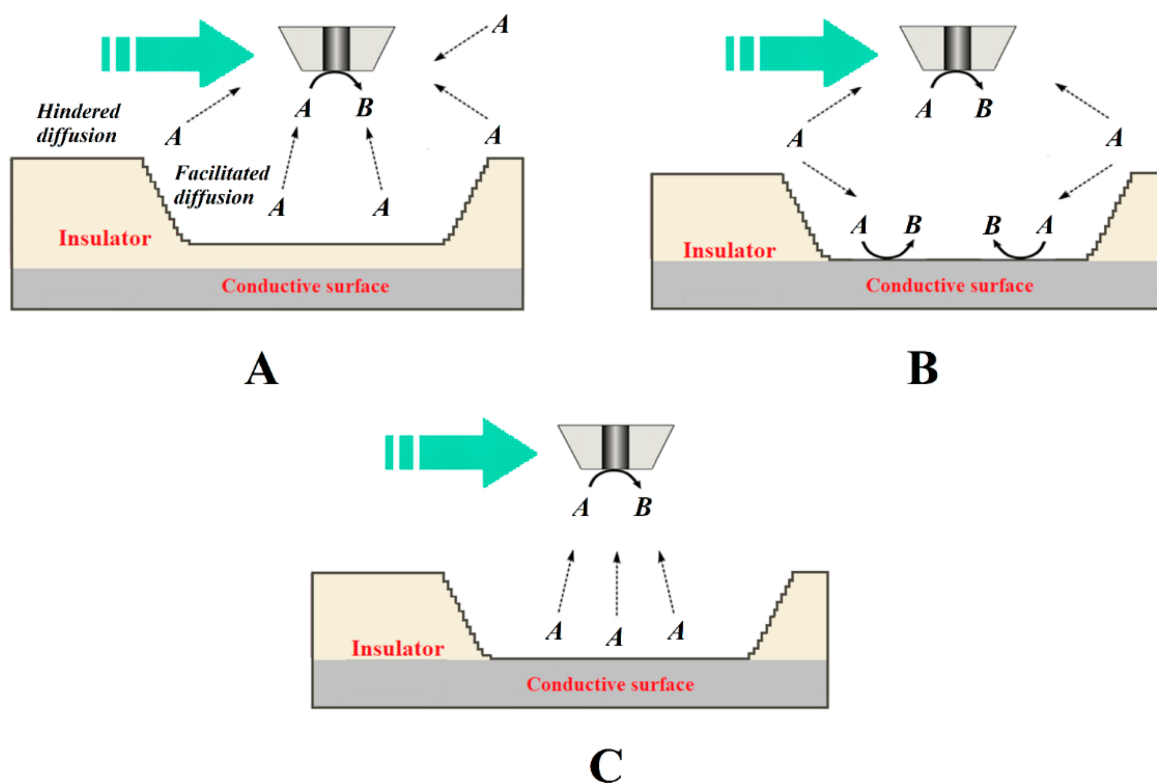


Figure 7. Diagrams of the processes that occur at the tip for the electrochemical conversion of species A to B when the tip passes over a larger defect depending on whether it is an insulating or a conductive surface exposed to the aqueous medium. The green arrow indicates the scan direction. Depending on the source of species A, the following situations have been described: **(A)** species A is present in the aqueous medium and is not consumed within the defect, which behaves as an insulator; **(B)** species A is present in the aqueous medium and transforms at both the tip and the bottom of the defect; and **(C)** species A is generated at the bottom of the defect, although it was not originally present in the aqueous environment.

This procedure required the choice of detection modes more sensitive to either the topographical changes or the chemical activity by controlling the local chemistry of the system and the characteristics of the tip, followed by a subsequent stage of recording the combined signal of the complete corroding system. This methodology can be further extended by combining potentiometric modes with amperometric operation using multi-probe configurations, as recently demonstrated of corrosion processes on cut edges of organically coated galvanized steel [11]. In this case, the combined amperometric/potentiometric SECM operation was performed by fabricating a multi-probe assembly using the same procedures previously developed for fabricating potentiometric probes with an internal reference electrode [9].

An alternate way to overcome the referred limitation is to associate SECM with other surface resolved techniques [51]. An option is the combination of SECM with AFM using cantilever probes modified for this purpose, which made it possible to simultaneously image the topography and the electrochemical activity in situ. In this way, the monitoring of nucleating corrosion pits in iron-based materials [52] and the dissolution-redeposition of metal ions in acidic environment [53] have been successfully imaged in situ.

Besides the combination of SECM with topographically sensitive techniques, software routines can be designed so that the scan is actually performed at a constant tip-substrate distance (i.e., following the actual surface of the sample) instead of operating at a constant height, as is normally done in conventional SECM operation [54]. Alternately, the measurement of shear forces between the tip and the surface can be used for constant distance operation in SECM instead of AFM [54]. The success of such an association was reported by Etienne et al. for monitoring the performance of self-healing coatings deposited on an aluminium alloy [55]. The local features with a depth profile in excess of 50 μm were successfully resolved. In addition, local chemical analysis was simultaneously performed using in situ Raman spectroscopy.

Finally, corrosion reactions that progress far beyond their initial stages and eventually reach dimensions of a hundred micrometers or a few millimeters are already accessible using other experimental techniques and would not require the micrometric resolution of SECM.

References

1. Santana, J.J.; Izquierdo, J. Souto, R.M.; Uses of Scanning Electrochemical Microscopy (SECM) for the Characterization with Spatial and Chemical Resolution of Thin Surface Layers and Coating Systems Applied on Metals: A Review. *Coatings* **2022**, *12*, 637, [10.3390/coatings12050637](https://doi.org/10.3390/coatings12050637).
2. Izquierdo, J.; Knittel, P.; Kranz, C.; Scanning electrochemical microscopy: an analytical perspective. *Analytical and Bioanalytical Chemistry* **2017**, *410*, 307-324, [10.1007/s00216-017-0742-7](https://doi.org/10.1007/s00216-017-0742-7).
3. Bard, A.J.; Fan, F.R.F.; Kwak, J.; Lev, O.; Scanning electrochemical microscopy. Introduction and principles. *Analytical Chemistry* **1989**, *61*, 132-138, [10.1021/ac00177a011](https://doi.org/10.1021/ac00177a011).
4. Etienne, M.; Schulte, A.; Schuhmann, W.; High resolution constant-distance mode alternating current scanning electrochemical microscopy (AC-SECM). *Electrochemistry Communications* **2004**, *6*, 288-293, [10.1016/j.elecom.2004.01.006](https://doi.org/10.1016/j.elecom.2004.01.006).
5. Kuznetsov, V.; Maljusch, A.; Souto, R.M.; Bandarenka, A.S.; Schuhmann, W; Characterisation of localised corrosion processes using scanning electrochemical impedance microscopy. *Electrochemistry Communications* **2014**, *44*, 38-41, [10.1016/j.elecom.2014.04.011](https://doi.org/10.1016/j.elecom.2014.04.011).
6. Lamaka, S.V.; Souto, R.M.; Ferreira, M.G.S.. Microscopy: Science, Technology, Applications and Education; Volume 3; Méndez-Vilas, A., Díaz, J., Eds.; Formatex Research Center: Badajoz, Spain, 2010; pp. 2162–2173.
7. Kiss, A.; Filotás, D.; Souto, R.M.; Nagy, G.; The effect of electric field on potentiometric Scanning Electrochemical Microscopic imaging. *Electrochemistry Communications* **2017**, *77*, 138-141, [10.1016/j.elecom.2017.03.011](https://doi.org/10.1016/j.elecom.2017.03.011).
8. Filotás, D.; Fernández-Pérez, B.M.; Izquierdo, J.; Kiss, A.; Nagy, L.; Nagy, G.; Souto; Improved potentiometric SECM imaging of galvanic corrosion reactions. *Corrosion Science* **2017**, *129*, 136-145, [10.1016/j.corsci.2017.10.006](https://doi.org/10.1016/j.corsci.2017.10.006).
9. Filotás, D.; Fernández-Pérez, B.M.; Kiss, A.; Nagy, L.; Nagy, G.; Souto, R.M.; Double Barrel Microelectrode Assembly to Prevent Electrical Field Effects in Potentiometric SECM Imaging of Galvanic Corrosion Processes. *Journal of The Electrochemical Society* **2018**, *165*, C270-C277, [10.1149/2.0671805jes](https://doi.org/10.1149/2.0671805jes).
10. Marques, A.G.; Izquierdo, J.; Souto, R.M.; Simões, A.M.; SECM imaging of the cut edge corrosion of galvanized steel as a function of pH. *Electrochimica Acta* **2015**, *153*, 238-245, [10.1016/j.electacta.2014.11.192](https://doi.org/10.1016/j.electacta.2014.11.192).
11. Filotás, D.; Izquierdo, J.; Fernández-Pérez, B.M.; Nagy, L.; Nagy, G.; Souto, R.M.; Contributions of Microelectrochemical Scanning Techniques for the Efficient Detection of Localized Corrosion Processes at the Cut Edges of Polymer-Coated Galvanized Steel. *Molecules* **2022**, *27*, 2167, [10.3390/molecules27072167](https://doi.org/10.3390/molecules27072167).
12. Stulík, K.; Amatore, C.; Holub, K.; Marecek, V.; Kutner, W.; Microelectrodes. Definitions, characterization, and applications (Technical report). *Pure and Applied Chemistry* **2000**, *72*, 1483-1492, [10.1351/pac200072081483](https://doi.org/10.1351/pac200072081483).
13. Izquierdo, J.; Nagy, L.; Varga, Á.; Santana, J.J.; Nagy, G.; Souto, R.M.; Spatially resolved measurement of electrochemical activity and pH distributions in corrosion processes by scanning electrochemical microscopy using antimony microelectrode tips. *Electrochimica Acta* **2011**, *56*, 8846-8850, [10.1016/j.electacta.2011.07.076](https://doi.org/10.1016/j.electacta.2011.07.076).
14. Zhu, Z.J.; Ye, Z.N.; Zhang, J.Q.; Cao, F.H.; Novel dual Pt-Pt/IrO ultramicroelectrode for pH imaging using SECM in both potentiometric and amperometric modes. *Electrochemistry Communications* **2018**, *88*, 47-51, [10.1016/j.elecom.2018.01.018](https://doi.org/10.1016/j.elecom.2018.01.018).
15. Varvara, S.; Caniglia, G.; Izquierdo, J.; Bostan, R.; Gaina, L.; Souto, R.M.; Multiscale electrochemical analysis of the corrosion control of bronze in simulated acid rain by horse-chestnut (*Aesculus hippocastanum* L.) extract as green inhibitor. *Corrosion Science* **2019**, *165*, 108381, [10.1016/j.corsci.2019.108381](https://doi.org/10.1016/j.corsci.2019.108381).
16. Filotás, D.; Asserghine, A.; Nagy, L.; Nagy, G.; Short-term influence of interfering ion activity change on ion-selective micropipette electrode potential; another factor that can affect the time needed for imaging in potentiometric SECM. *Electrochemistry Communications* **2017**, *77*, 62-64, [10.1016/j.elecom.2017.02.010](https://doi.org/10.1016/j.elecom.2017.02.010).
17. Kiss, A.; Nagy, G.; New SECM scanning algorithms for improved potentiometric imaging of circularly symmetric targets. *Electrochimica Acta* **2014**, *119*, 169-174, [10.1016/j.electacta.2013.12.041](https://doi.org/10.1016/j.electacta.2013.12.041).
18. Kiss, A.; Nagy, G.; Deconvolution of potentiometric SECM images recorded with high scan rate. *Electrochimica Acta* **2015**, *163*, 303-309, [10.1016/j.electacta.2015.02.096](https://doi.org/10.1016/j.electacta.2015.02.096).

19. Horrocks, B.R.; Mirkin, M.V.; Pierce, D.T.; Bard, A.J.; Nagy, G.; Toth, K.; Scanning electrochemical microscopy. 19. Ion-selective potentiometric microscopy. *Analytical Chemistry* **1993**, *65*, 1213-1224, [10.1021/ac00057a019](https://doi.org/10.1021/ac00057a019).
20. Frateur, I.; Bayet, E.; Keddam, M.; Tribollet, B.; Local redox potential measurement. *Electrochemistry Communications* **1999**, *1*, 336-340, [10.1016/s1388-2481\(99\)00066-1](https://doi.org/10.1016/s1388-2481(99)00066-1).
21. Filotás, D.; Fernández-Pérez, B.M.; Izquierdo, J.; Nagy, L.; Nagy, G.; Souto, R.M.; Novel dual microelectrode probe for the simultaneous visualization of local Zn²⁺ and pH distributions in galvanic corrosion processes. *Corrosion Science* **2017**, *114*, 37-44, [10.1016/j.corsci.2016.10.014](https://doi.org/10.1016/j.corsci.2016.10.014).
22. Souto, R.M.; Izquierdo, J.; Santana, J.J.; Kiss, A.; Nagy, L.; Nagy, G.. Current Microscopy Contributions to Advances in Science and Technology; Volume 2; Méndez-Vilas, A., Eds.; Formatex Research Center: Badajoz, Spain, 2012; pp. 1407–1415.
23. Santos, C.S.; Lima, A.S.; Battistel, D.; Daniele, S.; Bertotti, M.; Fabrication and Use of Dual-function Iridium Oxide Coated Gold SECM Tips. An Application to pH Monitoring above a Copper Electrode Surface during Nitrate Reduction.. *Electroanalysis* **2016**, *28*, 1441-1447, [10.1002/elan.201501082](https://doi.org/10.1002/elan.201501082).
24. Zhu, Z.J.; Liu, X.Y.; Ye, Z.N.; Zhang, J.Q.; Cao, F.H.; Zhang, J.X.; A fabrication of iridium oxide film pH micro-sensor on Pt ultramicroelectrode and its application on in-situ pH distribution of 316L stainless steel corrosion at open circuit potential. *Sensors and Actuators B: Chemical* **2018**, *255*, 1974-1982, [10.1016/j.snb.2017.08.219](https://doi.org/10.1016/j.snb.2017.08.219).
25. Kwak, J.; Bard, A.J.; Scanning electrochemical microscopy. Theory of the feedback mode. *Analytical Chemistry* **1989**, *61*, 1221-1227, [10.1021/ac00186a009](https://doi.org/10.1021/ac00186a009).
26. Souto, R.M.; González-García, Y.; González, S.; Burstein, G.T.; Damage to paint coatings caused by electrolyte immersion as observed in situ by scanning electrochemical microscopy. *Corrosion Science* **2004**, *46*, 2621-2628, [10.1016/j.corsci.2004.06.002](https://doi.org/10.1016/j.corsci.2004.06.002).
27. Souto, R.M.; González-García, Y.; González, S.; Evaluation of the corrosion performance of coil-coated steel sheet as studied by scanning electrochemical microscopy. *Corrosion Science* **2008**, *50*, 1637-1643, [10.1016/j.corsci.2008.02.019](https://doi.org/10.1016/j.corsci.2008.02.019).
28. Elkebir, Y.; Mallarino, S.; Trinh, D.; Touzain, S.; Effect of physical ageing onto the water uptake in epoxy coatings. *Electrochimica Acta* **2020**, *337*, 135766, [10.1016/j.electacta.2020.135766](https://doi.org/10.1016/j.electacta.2020.135766).
29. Duarte, R.G.; González, S.; Castela, A.S.; Ferreira, M.G.S.; Souto, R.M.; Sensing polymer inhomogeneity in coated metals during the early stages of coating degradation. *Progress in Organic Coatings* **2012**, *74*, 365-370, [10.1016/j.porgcoat.2011.11.009](https://doi.org/10.1016/j.porgcoat.2011.11.009).
30. Souto, R.M.; González-García, Y.; González, S.; Imaging the Origins of Coating Degradation and Blistering Caused by Electrolyte Immersion Assisted by SECM. *Electroanalysis* **2009**, *21*, 2569-2574, [10.1002/elan.200900262](https://doi.org/10.1002/elan.200900262).
31. Souto, R.M.; González-García, Y.; Izquierdo, J.; González, S.; Examination of organic coatings on metallic substrates by scanning electrochemical microscopy in feedback mode: Revealing the early stages of coating breakdown in corrosive environments. *Corrosion Science* **2010**, *52*, 748-753, [10.1016/j.corsci.2009.10.035](https://doi.org/10.1016/j.corsci.2009.10.035).
32. Vosgien-Lacombe, C.; Bouvet, G.; Trinh, D.; Mallarino, S.; Touzain, S.; Effect of pigment and temperature onto swelling and water uptake during organic coating ageing. *Progress in Organic Coatings* **2018**, *124*, 249-255, [10.1016/j.porgcoat.2017.11.022](https://doi.org/10.1016/j.porgcoat.2017.11.022).
33. Trinh, D.; Vosgien-Lacombe, C.; Bouvet, G.; Mallarino, S.; Touzain, S.; Use of ionic liquids in SECM experiments to distinguish effects of temperature and water in organic coating swelling. *Progress in Organic Coatings* **2019**, *139*, 105438, [10.1016/j.porgcoat.2019.105438](https://doi.org/10.1016/j.porgcoat.2019.105438).
34. Battistel, D.; Daniele, S.; Gerbasi, R.; Baldo, M.A.; Characterization of metal-supported Al₂O₃ thin films by scanning electrochemical microscopy. *Thin Solid Films* **2010**, *518*, 3625-3631, [10.1016/j.tsf.2009.09.080](https://doi.org/10.1016/j.tsf.2009.09.080).
35. Izquierdo, J.; Bolat, G.; Cimpoesu, N.; Trinca, L.C.; Mareci, D.; Souto, R.M.; Electrochemical characterization of pulsed layer deposited hydroxyapatite-zirconia layers on Ti-21Nb-15Ta-6Zr alloy for biomedical application. *Applied Surface Science* **2016**, *385*, 368-378, [10.1016/j.apsusc.2016.05.130](https://doi.org/10.1016/j.apsusc.2016.05.130).
36. Carbonell, D.J.; García-Casas, A.; Izquierdo, J.; Souto, R.M.; Galván, J.C.; Jiménez-Morales, A.; Scanning electrochemical microscopy characterization of sol-gel coatings applied on AA2024-T3 substrate for corrosion protection. *Corrosion Science* **2016**, *111*, 625-636, [10.1016/j.corsci.2016.06.002](https://doi.org/10.1016/j.corsci.2016.06.002).
37. Cornut, R.; Lefrou, C.; New analytical approximation of feedback approach curves with a microdisk SECM tip and irreversible kinetic reaction at the substrate. *Journal of Electroanalytical Chemistry* **2008**, *621*, 178-184, [10.1016/j.jelechem.2007.09.021](https://doi.org/10.1016/j.jelechem.2007.09.021).
38. Mansikkamäki, K.; Ahonen, P.; Fabricius, G.; Murtomäki, L.; Kontturi, K.; Inhibitive Effect of Benzotriazole on Copper Surfaces Studied by SECM. *Journal of The Electrochemical Society* **2005**, *152*, B12-B16, [10.1149/1.1829413](https://doi.org/10.1149/1.1829413).

39. Mansikkamaki, K.; Haapanen, U.; Johans, C.; Kontturi, K.; Valden, M.; Adsorption of Benzotriazole on the Surface of Copper Alloys Studied by SECM and XPS. *Journal of The Electrochemical Society* **2006**, *153*, B311-B318, [10.1149/1.2208912](#).
40. Izquierdo, J.; Santana, J.J.; González, S.; Souto, R.M.; Uses of scanning electrochemical microscopy for the characterization of thin inhibitor films on reactive metals: The protection of copper surfaces by benzotriazole. *Electrochimica Acta* **2010**, *55*, 8791-8800, [10.1016/j.electacta.2010.08.020](#).
41. Izquierdo, J.; Santana, J.J.; González, S.; Souto, R.M.; Scanning microelectrochemical characterization of the anti-corrosion performance of inhibitor films formed by 2-mercaptobenzimidazole on copper. *Progress in Organic Coatings* **2012**, *74*, 526-533, [10.1016/j.porgcoat.2012.01.019](#).
42. Zoski, C.G.; Review—Advances in Scanning Electrochemical Microscopy (SECM). *Journal of The Electrochemical Society* **2015**, *163*, H3088-H3100, [10.1149/2.0141604jes](#).
43. Radtke, V.; Heß, C.; Souto, R.M.; Heinze, J.; Electroless, Electrolytic and Galvanic Copper Deposition with the Scanning Electrochemical Microscope (SECM). *Zeitschrift für Physikalische Chemie* **2006**, *220*, 393-406, [10.1524/zpch.2006.220.4.393](#).
44. Leonard, K.C.; Bard, A.J.; The Study of Multireactional Electrochemical Interfaces via a Tip Generation/Substrate Collection Mode of Scanning Electrochemical Microscopy: The Hydrogen Evolution Reaction for Mn in Acidic Solution. *Journal of the American Chemical Society* **2013**, *135*, 15890-15896, [10.1021/ja407395m](#).
45. Eckhard, K.; Chen, X.; Turcu, F.; Schuhmann, W.; Redox competition mode of scanning electrochemical microscopy (RC-SECM) for visualisation of local catalytic activity. *Physical Chemistry Chemical Physics* **2006**, *8*, 5359-5365, [10.1039/b609511a](#).
46. Souto, R.M.; Fernández-Mérida, L.; González, S.; SECM Imaging of Interfacial Processes in Defective Organic Coatings Applied on Metallic Substrates Using Oxygen as Redox Mediator. *Electroanalysis* **2009**, *21*, 2640-2646, [10.1002/elan.200900232](#).
47. Bastos, A.C.; Simões, A.M.; González, S.; González-García, Y.; Souto, R.M.; Application of the scanning electrochemical microscope to the examination of organic coatings on metallic substrates. *Progress in Organic Coatings* **2005**, *53*, 177-182, [10.1016/j.porgcoat.2005.02.005](#).
48. da Silva, R.M.P.; Izquierdo, J.; Milagre, M.X.; Betancor-Abreu, A.M.; de Oliveira, L.A.; Antunes, R.A.; Souto, R.M.; Costa, I.; On the local corrosion behavior of coupled welded zones of the 2098-T351 Al-Cu-Li alloy produced by Friction Stir Welding (FSW): An amperometric and potentiometric microelectrochemical investigation. *Electrochimica Acta* **2021**, *373*, 137910, [10.1016/j.electacta.2021.137910](#).
49. Frateur, I.; Huang, V.M.-W.; Orazem, M.E.; Pébère, N.; Tribollet, B.; Vivier, V.; Local electrochemical impedance spectroscopy: Considerations about the cell geometry. *Electrochimica Acta* **2008**, *53*, 7386-7395, [10.1016/j.electacta.2008.01.012](#).
50. Souto, R.M.; Santana, J.J.; Fernández-Mérida, L.; González, S.; Sensing electrochemical activity in polymer coated metals during the early stages of coating degradation-Effect of the polarization of the substrate. *Electrochimica Acta* **2011**, *56*, 9596-9601, [10.1016/j.electacta.2011.03.077](#).
51. Kranz, C.; Recent advancements in nanoelectrodes and nanopipettes used in combined scanning electrochemical microscopy techniques. *The Analyst* **2013**, *139*, 336-352, [10.1039/c3an01651j](#).
52. Izquierdo, J.; Eifert, A.; Kranz, C.; Souto, R.M.; In Situ Monitoring of Pit Nucleation and Growth at an Iron Passive Oxide Layer by using Combined Atomic Force and Scanning Electrochemical Microscopy. *ChemElectroChem* **2015**, *2*, 1847-1856, [10.1002/celc.201500100](#).
53. Izquierdo, J.; Eifert, A.; Kranz, C.; Souto, R.M.; In situ investigation of copper corrosion in acidic chloride solution using atomic force—scanning electrochemical microscopy. *Electrochimica Acta* **2017**, *247*, 588-599, [10.1016/j.electacta.2017.07.042](#).
54. Schulte, A.; Shuhmann, W.. Science, Technology and Education of Microscopy: An Overview; Méndez-Vilas, A.; Díaz, J., Eds.; Formatex Research Center: Badajoz, Spain, 2003; pp. 753–760.
55. Etienne, M.; Dossot, M.; Grausem, J.; Herzog, G.; Combined Raman Microspectrometer and Shearforce Regulated SECM for Corrosion and Self-Healing Analysis. *Analytical Chemistry* **2014**, *86*, 11203-11210, [10.1021/ac502670t](#).